The 14th World Conference on Earthquake Engineering
October 12-17, 2008, Beijing, China

ANALYSIS, TESTING, DESIGN AND CONSTRUCTION OF A BASE-ISOLATED/SUPPLEMENTALLY DAMPED BUILDING

S. Sorace[1] and G. Terenzi[2]

[1] *Associate Professor, Dept. of Civil Engineering and Architecture, University of Udine, Udine, Italy*
[2] *Researcher, Dept. of Civil and Environmental Engineering, University of Florence, Florence, Italy*
Email: stefano.sorace@uniud.it, terenzi@dicea.unifi.it

ABSTRACT:

The first actual application to a demonstrative strategic building of a special base isolation/supplemental damping system, where fluid viscous spring-dampers are coupled to steel-Teflon sliders, is presented in this paper. The results of a testing campaign aimed at assessing the interference of the dissipative actions of the two component devices, as a final step of the research studies previously developed by the authors on this technology, are summed up. The design and performance evaluation analyses carried out on the building are then discussed. Highlights of the construction works and technical installation details are finally illustrated.

KEYWORDS: Advanced seismic protection, Base isolation, Damping, Testing, Design.

1. INTRODUCTION

Base isolation and supplemental damping represent the standard passive control strategies in advanced seismic protection of building structures. The two strategies direct to clearly distinct design philosophies and practical applications. The sole interaction between them is that some additional damping is always required in base isolation, so that the displacements in the mobile plane are kept below acceptable limits. In this respect, dissipative isolators, like the high damping rubber bearings in widespread use, ensure reasonably good performance. Nonetheless, they feature two well-known limits, and namely: for considerably irregular buildings in plan, the torsion response effects induced by seismic action are not easily constrained; the maximum equivalent damping now offered by commercial devices is generally no greater than 15–16%, to which relatively high base displacements often correspond (about 200-300 mm and higher), for standard buildings as well.
With the aim of improving performance further, combined base isolation/supplemental damping (BISD) systems have been implemented by assembling various types of sliders and dissipaters. A special BISD system belonging to this class, where fluid viscous (FV) pressurized spring-dampers are coupled to steel-Teflon (ST) sliding bearings, has been studied by the authors for several years (Sorace and Terenzi 2001, Sorace et al 2008). As a final step of these studies, a pilot application of the BISD system was recently completed, by incorporating the system at the base of a demonstrative strategic public building in the neighborhood of Florence. This application makes an absolute novelty in Italy—where the total number of base isolated structures, either already built or under construction, exceeds 90 buildings, all of which include rubber bearings, in several cases coupled with steel-Teflon sliders or articulated steel sledges—, and in the rest of Europe.

2. ST SLIDERS AND FV SPRING-DAMPERS

2.1. ST Sliders

Steel-Teflon sliders behave as pure friction elements characterized by very low values of the friction coefficient μ. This coefficient depends on the quality of manufacturing, and particularly of the mirror finish in the austenitic steel plate interfacing the Teflon disk, as well as of the lubricant with which the disk is imbued (generally, a silicone oil). Moreover, μ depends on deformation velocity and normal pressure. Actually, the strict prescriptions governing manufacturing and lubrication of this class of sliders result in a very limited dependence on the former parameter in dynamic response conditions. This was confirmed by an experimental

campaign reported in (Sorace et al 2008), which highlighted nearly constant μ values starting from a velocity of around 10 mm/s. Some decrease is normally observed for lower velocities, and more appreciable falls (by about 2) are seen only in static tests.
A schematic cross section of the largest-sized sliders mounted in the pilot building in Florence (M 1400, where the number indicates, in kN units, the maximum allowable normal force under vertical loads, *V*), and a photographic view taken during the installation of one of these bearings, are illustrated in Figure 1. The other two types of sliders (M 600, and M 1000) only differ in the dimensions in plan of the square Teflon disk, and relevant top and bottom plates.

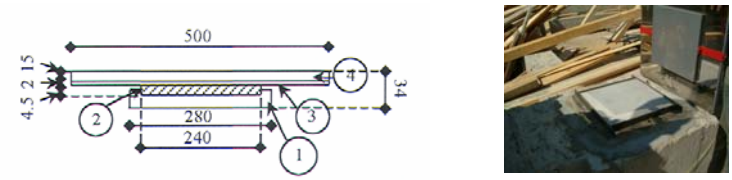

Figure 1 Cross section (1. square stainless steel bottom plate; 2. lubricated square Teflon disk; 3. austenitic steel sheet; 4. square stainless steel top plate – dimensions in millimeters) and view of a M 1400 ST slider

2.2. FV Spring-Dampers

The pressurized fluid viscous devices adopted in this project (Jarret SL 2008), whose schematic cross section is illustrated in Figure 2, are characterized by very low values—ranging from 0.1 to 0.2—of the fractional exponent α of the power law expressing their damping reaction force as a function of the relative velocity between the device ends. In fact, these values ensure the highest normalized damping capacity and, at the same time, identify the lowest dependence on velocity of this type of dissipaters within the general class of non-linear viscous devices. This is justified by the special flowing mechanism of the highly viscous silicone elastomer contained in the inner casing of the device, which flows through a very narrow annular space between the casing surface and the piston head (Figure 2). The pressurization of the casing, guaranteed by a pre-load applied upon manufacturing, ensures total self-centering capacity of the device.

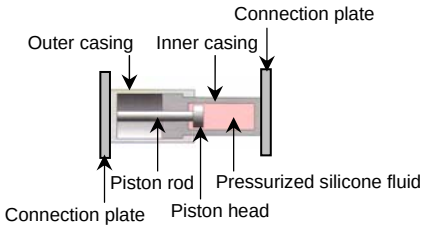

Figure 2 Cross section of a FV spring-damper

Further information on the mechanical properties of the devices, including their strain-rate dependency, as well as on their analytical/numerical modeling, can be found in (Sorace and Terenzi 2001, 2008a).

3. NEW EXPERIMENTAL CAMPAIGN ON THE BISD SYSTEM

A laboratory installation of a complete BISD system has been recently accomplished at the ELSA laboratory of the Joint Research Centre (Ispra, Italy), to develop a new comprehensive experimental program on this technology (Sorace et al 2008). A task of this program consisted in a set of cyclic characterization tests, aimed at estimating the possible interferences—implicitly assumed to be null in relevant analytical and computational models—of the frictional response of ST sliders with the damping action of FV dissipaters. A scheme and a photographic view of the experimental setup are shown in Figure 3. Several sets of cyclic tests were carried out by varying the vertical loads applied by the static actuators, and the input velocities imposed by the dynamic actuators. As an example of the experimental results, the force-displacement cycles and the energy time-histories derived from the test developed with a normal stress on the sliders equal to 9.2 MPa, and a

velocity of 63 mm/s, are plotted in Figure 4.

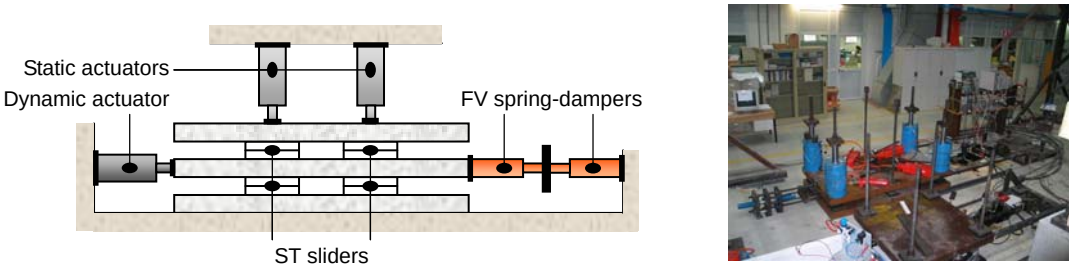

Figure 3 Scheme and view of the experimental setup for the tests on the BISD system

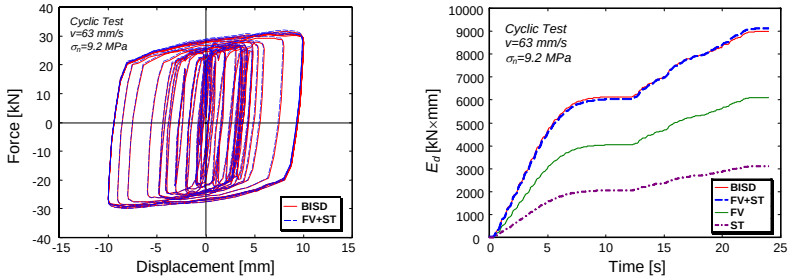

Figure 4 Force-displacement cycles and energy time-histories obtained from cyclic tests on the BISD system and from corresponding tests on the component devices

In the first graph in Figure 4, the cycles of the assembled system are compared to the cycles obtained as the sum of the contributions provided by the FV spring-dampers and the ST sliders tested separately, denoted by symbol "FV+ST". The same comparison is also illustrated in the energy graph, where the response time-histories of the sliders and the dissipaters alone are plotted too. These figures clearly show that the sum of the contributions in terms of reaction forces and dissipated energy of the two component devices taken separately coincides with the corresponding global measure for the system. These data are confirmed by the tests carried out with all the remaining normal stress and velocity values, and corroborate the hypothesis of a linear additive combination of the dissipative actions of the two types of devices in this mixed installation. Concerning the relative energy contributions of the sliders and the dissipaters shown in the graph in Figure 4, they strictly depend on the characteristics of the test performed, in particular on the maximum displacement imposed. The relatively small displacements applied in this experimental program (equal to ±10 mm, which approximately coincide with the values induced by the serviceability design earthquake on the building in Florence, as defined in the following section), give rise to a lower energy contribution of the FV devices—in this case equal to 2/3 of the total dissipated energy—as compared to when larger displacements are reached, as in a corresponding basic design input earthquake.

4. APPLICATION OF THE BISD SYSTEM TO A DEMONSTRATIVE BUILDING

4.1. Design Earthquake Levels and Seismic Performance Objectives

The building considered here, i.e. the new site of a no-profit association offering social services, and station of the emergency vehicles of the local civil protection headquarters, is considerably irregular in plan and height. According to the Italian territory classification provided for by the edition of the Seismic Standards in force when the design was developed (OPCM-3431 2005), the building is situated in seismic zone 2, like the whole city of Florence and its hinterland. The peak ground acceleration assigned to the basic design earthquake (BDE, characterized by 10% probability of being exceeded over 50 years) for this zone is equal to 0.25 g (2.45 m/s^2), for rock-soil conditions ("A"-soil type). The foundation soil of the building was evaluated to be "C" type (medium-density clay), based on the results of geological and geotechnical investigations, including down-hole

tests. A soil-factor S=1.25 was consequently introduced to multiply the "A"-soil ground acceleration. Moreover, an importance factor γ_I=1.2 was applied, to account for the use of the building. The corresponding elastic pseudo-acceleration response spectrum at 5% viscous damping adopted by the referred Italian seismic Standards for base-isolated building structures (with increased spectral ordinates in the medium-to-high period zone, as compared to the spectrum assumed for non-isolated structures) is plotted in Figure 5. In total, a BDE peak amplitude of 0.375 g (3.68 m/s^2), hereafter denoted as $A_{i,n}$, was adopted in the analyses. This design level, combined with the structural irregularity and the strategic role of the building, qualified it as a suitable candidate for a demonstrative application of the BISD technology.

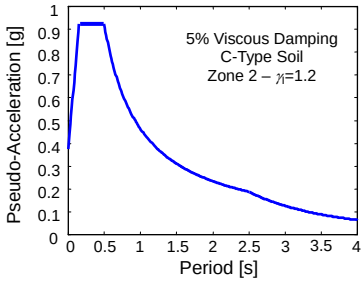

Figure 5 Elastic pseudo-acceleration response spectrum adopted in the design

An "immediate occupancy" performance level, with no damage to the superstructure members and negligible local damages to internal partitions and finishes, was assumed as design objective for the response to the BDE. In addition to the BDE, two further levels of seismic action were considered: a serviceability design earthquake (SDE, with a 50% probability of exceedence over 50 years), with a factor 0.4 on the BDE amplitude, for the analyses at the damage limit state, as required by Italian Standards (OPCM-3431 2005); and a maximum considered event (MCE, with a 2% probability of exceedence over 50 years), with a factor 1.5 on the BDE amplitude, for the analyses at the collapse limit state. A "fully operational" performance level is imposed for the response to SDE by (OPCM-3431 2005), which is assessed by a limit interstory drift equal to 0.75% of story height, when infills are not in contact with the frame structure elements (as in this design). On the other hand, the MCE was deliberately introduced to check the effectiveness of the protective system also under this hypothetical extreme input level for the building site. For this level, the maximum base displacement was assumed to be lower than the available piston stroke of the spring-dampers, and the superstructure was assumed to satisfy the requirements of a "damage control" performance objective, with at most some slight plasticization in few beams and no plasticization in columns.

4.2. Plan Arrangement of Protection System and Adopted Devices

Figure 6 shows the plan of the mobile (basement) floor, where the locations of the four plus four pairs of spring-dampers placed along each of the two main directions in plan—x and y—are highlighted with circles (devices Jx1-Jx8) and squares (devices Jy1-Jy8). Two photographic views taken during the finishing works of the building are also displayed in Figure 6. The locations of the FV devices were derived from a best positioning search process aimed at minimizing the distance between centre of mass and centre of stiffness of the superstructure. The constraints of this process were represented by the plot of the main superstructure frames (all aligned along the y axis), and relevant foundation beams. The final solution was a nearly complete superimposition along x, and a distance of about 90 cm along y. The ST bearings were placed below each one of the thirty-one columns, plus the bottom-stroke slab of the lift-shaft (four M 1400, eighteen M 1000 and ten M 600 elements mentioned in a section above were introduced in total). A fundamental vibration period of the isolated structure equal to 2 s was targeted for the strongest direction y.

The preliminary design phase, described in detail in (Sorace and Terenzi 2008b) led to select the following value of the damping coefficient of the FV spring-dampers: c = 287 kN·(s/m)$^{0.15}$. This value is supplied by a medium-sized FV device in standard production (Jarret SL 2008), characterized by a maximum energy dissipation capacity of 100 kJ, a maximum piston displacement of 200 mm (±100 mm in half-stroke initial configuration), and a spring component stiffness that ensures attainment of the above-mentioned target fundamental period along y (a period of 2.2 s comes out along the weakest direction x).

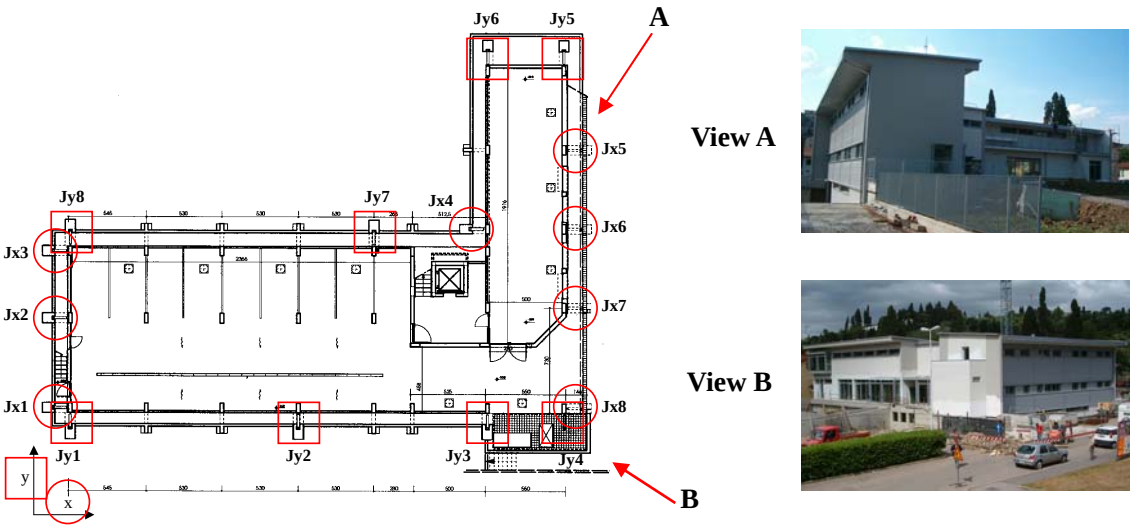

Figure 6 Plan of the mobile floor, and views of the building during the finishing works

4.3. Final Design Phase

A non-linear dynamic approach was adopted in the final verification phase by using five artificial accelerograms generated from the response spectrum shown in Figure 5 as inputs. The finite element model for the structural analysis was generated by the SAP2000NL calculus code (CSI 2007). The library of this program includes a "friction isolator" finite element based on the Coulomb model, which effectively reproduces the behavior of the sliding bearings. Concerning the spring-dampers, non-linear spring and "dashpot" elements, whose reaction forces are expressed by relations 1 and 2, respectively, are also incorporated in SAP2000NL program. The computational model of fluid viscous devices, displayed in Figure 7, is completed by two further elements placed in parallel, i.e. a "gap" and a "hook", adopted to disconnect the spring-dampers when stressed in tension, and to stop them when the maximum stroke is reached, respectively. Finally, the static pre-load F_0 applied to the devices upon manufacturing is imposed, as an internal force, to a bar linking the four parallel elements to the external support. The complete finite element model of the building is also shown in Figure 7.

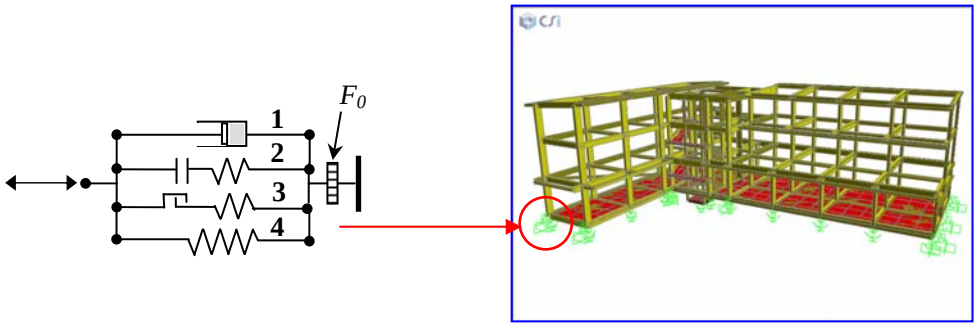

Figure 7 Computational model of a spring-damper (1. non-linear dashpot; 2. gap; 3. hook; 4. non-linear spring), and finite element model of the building

A synthesis of the results of the final verification design analyses is reported in the graphs in Figure 8, all of which referred to the response obtained from the most demanding of the five normative artificial accelerograms (the results were very similar for the five signals, with maximum relative differences not exceeding 3%). The graph on the left shows displacement time-histories of Jy1 and Jy5 spring-dampers for the BDE event, which prompt the two following observations. First, the values of maximum displacements are very low, and they do not exceed 40 mm. Slightly higher values come out in the x direction, although limited below 45 mm. This underlines the excellent performance of the system in terms of base displacements, which also allows adopting

simple and inexpensive connections for all utilities (gas, water, electricity), as illustrated below. The second observation regards the correlation of the two time-histories, quantified by a maximum difference lower than 10 mm. Considering that Jy1 and Jy5 spring-dampers are situated at two opposite ends in plan along the y axis, at a distance of 35 meters, this confirms that torsion response effects were satisfactorily restrained also for the component of seismic action parallel to this direction (the effects induced by the x component were virtually null). Concerning base shear, it can also be noted that the maximum values of the components along x and y correspond to peak base accelerations equal to 0.151 g and 0.177 g, respectively, for the most demanding accelerogram. This underlines the benefits of the protection system, ensuring 2.48 and 2.12 reduction factors on response accelerations as compared to peak ground acceleration. Thanks to such great filtering action of the protective system, no shear walls were required for the R/C superstructure, which consisted in a simple framed skeleton.

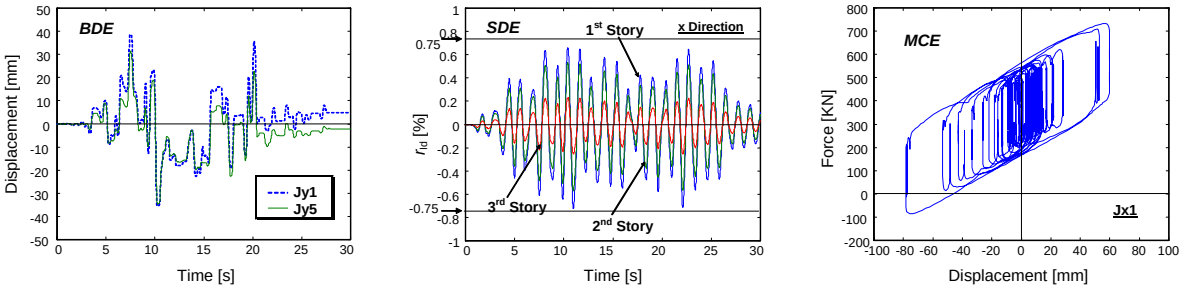

Figure 8 Displacement time-histories of Jy1 and Jy5 spring-dampers, for the BDE; normalised inter-story drift time-histories for the SDE; and response cycles of Jx1 spring-damper for the MCE

The central graph in Figure 8 shows the r_{Id} inter-story drift time-histories of the three stories, normalized to their respective inter-story heights, as calculated for the SDE and the weakest direction x. Maximum r_{Id} values equal to 0.7% are observed in the first story, and they are below the above-mentioned admissible threshold of 0.75% imposed by Italian Standards for the corresponding damage limit condition. Remarkably lower peak r_{Id} values emerge for the second and third floor, as well as for the stiffest direction y, giving rise to a satisfactory performance also at this level of input seismic action. The right graph in Figure 8 contains force-displacement hysteresis cycles of the most stressed Jx1 spring-damper for the MCE, which produces slightly higher displacements along x, as previously observed for the BDE. The peak values recorded for Jx1, equal to around 78 mm in absolute value, are considerably lower than the available piston stroke of ±100 mm. This ensures full operation of the protection system, as well as a totally elastic response of the superstructure, and the damage control performance objectives postulated for the MCE hazard level are therefore met.

Among several checks carried out within this final verification phase, two are discussed below. The first was aimed at assessing the influence of the damping coefficient choice on the performance of the isolation system—by means of base displacement—and the superstructure—by base shear. As illustrated in Figure 9, again referred to the BDE and the weakest x direction, the c_{des} value selected within the preliminary design phase corresponds to the lowest zone of the base shear-damping coefficient curve, and at the same time it ensures the low base displacements discussed above.

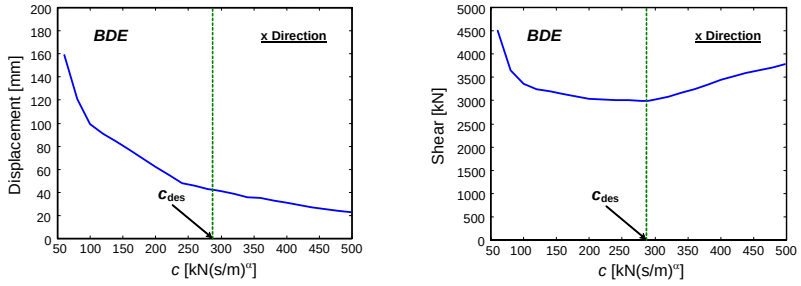

Figure 9 Base displacement and base shear as a function of damping coefficient

A progressively greater response in terms of base shear is obtained by increasing *c*. At the same time, acceptably low displacements (i.e. limited to around 60 mm, in order to exploit the special capabilities of the BISD system in controlling this parameter) are obtained for *c* values up to 50% lower than c_{des}. By cross-examining the data in Figure 9, the design *c* value proves to guarantee a satisfactory mixed control of base displacement and shear.
The second check consisted in an additional enquiry developed by several near-fault real ground motions recorded during the greatest earthquakes in Italy over the latest thirty years, to produce highly demanding response conditions for the base-isolated building. The N-S fault-normal main shock component recorded in Calitri station during an earthquake in Southern Italy on November 23, 1980 proved to be the most demanding among these ground motions. Calitri record is characterized by a distance of 8.8 km from the surface projection of the causative fault, magnitude M=6.3, and peak ground displacement, velocity and acceleration of 0.07 m, 0.23 m/s and 1.78 m/s^2. Moreover, the highest spectral ordinates of this signal fall within the range of 0.95 Hz to 0.65 Hz, which is the closest to the first vibration frequency of the isolated building among the considered set of Italian earthquake records with $M \geq 6$. The results of the analysis are summed up in Figure 10, where the Jx1 displacement and base shear time-histories along the x axis are graphed.

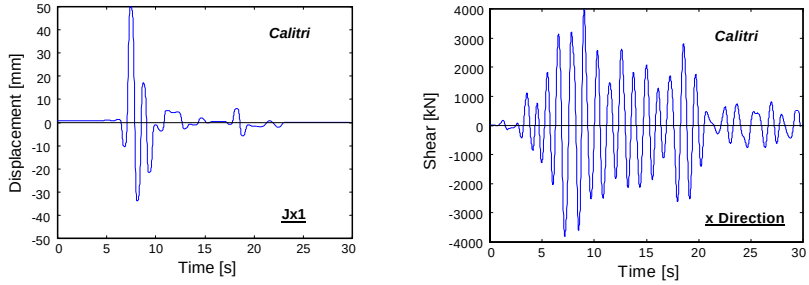

Figure 10 Jx1 displacement and base shear time-histories for Calitri ground motion

The peak Jx1 displacement (49.8 mm) and base shear (3990 kN) along x are 10% higher than the corresponding maximum values obtained from the analyses with the BDE-scaled normative accelerograms. On the other hand, the latter produce a considerably greater number of minor cycles, and thus a correspondingly higher amount of dissipated energy. This is due to their several comparable acceleration peaks, in place of the single more pronounced positive and negative peaks of the 1980 Calitri time-history.
Some photographic images referred to construction details peculiar to this specific design, are offered below. The location of one of sixteen steel spacers substituting the FV spring-dampers during the construction phases of the mobile floor, and the corresponding device after installation, are visualized in Figure 11. The spacers, which have the same length as the spring-dampers with the piston positioned at half stroke (1654 mm, with a 1 mm tolerance), are introduced to save this distance between the edges of the basement floor and the spring-damper buttresses during casting. This allows achieving a “mechanically precise” installation of the dissipaters after the completion of the mobile floor.

Figure 11 View of a steel spacer and the corresponding spring-damper, before and after the installation of the latter

Figure 12 illustrates the simple flexible joints installed on gas and water pipes, as well as on drain-pipes in the interfacing zones between the retaining walls and the building. These joints, capable of accommodating the

maximum nominal displacement of the FV spring-dampers, equal to ±100 mm, are in current production and do not cause any additional costs, as compared to the conventional joints mounted in standard fixed-base buildings.

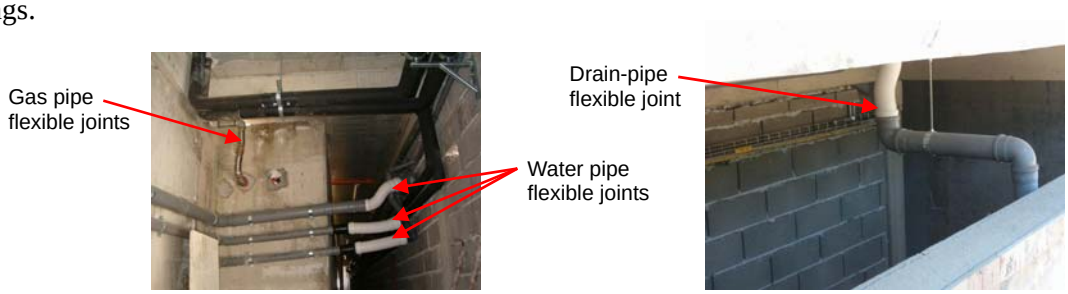

Figure 12 Details of the flexible joints installed on gas and water pipes, and drain-pipes

5. CONCLUDING REMARKS

The first application to an actual building of the seismic protection technology discussed in this paper confirmed its capacity to reach the high performance levels predicted by the theoretical, numerical and experimental studies previously carried out. The hypothesis of a linear combination of the dissipative contributions of FV spring-dampers and ST sliders was verified by the testing campaign developed to this aim, which allowed validating relevant numerical and computational models. All the performance objectives postulated for the two normative design seismic levels and the additional maximum considered event were largely met. The analyses carried out by the most demanding Italian historical near-fault ground motion considered in the design verification stage resembled the maximum response parameters derived from the BDE-scaled normative input motions, but with a lower damping demand due to the reduced number of acceleration peaks. The performance capacities of the BISD system highlighted for this building are not strictly related to its geometrical and morphological characteristics, as they totally confirm the results of a set of simulated designs previously carried out for R/C and steel structures with rather different configurations.

ACKNOWLEDGEMENTS

The study reported in this paper was financed by the Italian Department of Civil Protection within the Reluis-DPC Project 2005/2008. The authors gratefully acknowledge this financial support.

REFERENCES

CSI (2007). SAP2000NL, Structural Analysis Programs – Theoretical and Users Manual, Version No. 10.13, Berkeley, CA.
Jarret SL (2008). Shock-control technologies, URL http://www.introini.info.
OPCM-3431 (2005). Technical Standards for the design, evaluation and seismic retrofit of buildings (in Italian), Ministry of Public Works, Rome, Italy.
Sorace, S. and Terenzi, G. (2001). Non-linear dynamic modelling and design procedure of FV spring-dampers for base isolation. *Engineering Structures* **23:12**, 1556-67.
Sorace, S. and Terenzi, G. (2008a). Seismic protection of frame structures by fluid viscous damped braces. *Journal of Structural Engineering ASCE* **134:1**, 45-55.
Sorace, S. and Terenzi, G. (2008b). Analysis and demonstrative application of a base isolation/supplemental damping technology. *Earthquake Spectra* **24:3** (in print).
Sorace, S., Terenzi, G., Magonette, G. and Molina, F. J. (2008). Experimental investigation on a base isolation system incorporating steel-Teflon sliders and pressurized fluid viscous spring dampers. *Earthquake Engineering and Structural Dynamics* **37:2**, 225-242.